Journal of the American College of Cardiology Vol. 49, No. 13, 2007

Published by Elsevier Inc.
ISSN 0735-1097/07/$32.00
doi:10.1016/j.jacc.2007.01.059

Cardiac Imaging

Automated Analysis of Myocardial Deformation at Dobutamine Stress Echocardiography

An Angiographic Validation

Charlotte Bjork Ingul, MD,*† Asbjorn Stoylen, MD, PHD,* Stig A. Slordahl, MD, PHD,* Rune Wiseth, MD, PHD,* Malcolm Burgess, MD,† Thomas H. Marwick, MD, PHD†

Trondheim, Norway; and Brisbane, Australia

Objectives We investigated the accuracy of automated analysis of myocardial deformation during dobutamine stress echocardiography (DSE).

Background The time required for segmental measurement of strain rate imaging (SRI) limits its feasibility for quantification of DSE.

Methods Myocardial deformation was assessed at DSE in 197 patients, 76 with and 61 without coronary artery disease (CAD) at angiography, and 60 at low risk of CAD. Automated deformation analysis was based on velocity gradient and segment length methods of measuring longitudinal motion within a region of interest tracked through the cardiac cycle. Results were compared with independent wall motion scoring (WMS). Patients were randomly divided; group A (n = 69) established optimal cutoffs for the parameters and group B (n = 68) tested their accuracy.

Results The feasibility of WMS exceeded that of both SRI methods at rest and at peak stress. In group A, the area under the receiver-operating characteristics curve of the peak systolic strain rate was 0.90 by both methods, and the optimal cutoffs for detection of CAD were -1.3 (velocity gradient) and $-1.2\ s^{-1}$ (segment length). The areas under the receiver-operating characteristics curves for end-systolic strain were less (0.87) by both methods, with respective cutoffs of 9% and 8%. In group B, the velocity and segment length methods had respective sensitivities of 87% and 84% for SR, and 87% and 88% for end-systolic strain. Both significantly exceeded that of WMS in the same group (75%).

Conclusions Automated analysis of myocardial deformation at DSE is feasible and accurate, and may increase the sensitivity of expert conventional reading. (J Am Coll Cardiol 2007;49:1651–9) © 2007 by the American College of Cardiology Foundation

To attain published levels of accuracy, the interpretation of dobutamine stress echocardiography (DSE) requires an expert observer (1). A quantitative tool could reduce this dependence and help overcome the limitations of wall motion analysis. Quantitation using tissue Doppler measurements (e.g., peak systolic velocity and displacement) is feasible during DSE and provides modest accuracy (2–6), but is limited by the influence of adjacent segments. Measurement of deformation with longitudinal strain (S) and strain rate (SR) has been shown to be accurate in a small study of 44 patients (7). The lack of publication of further or larger studies about the accuracy of strain rate imaging (SRI) in DSE, or indeed its adoption as a clinical tool, may reflect the time requirement for image processing. Automated postprocessing would facilitate the uptake of SRI as a practical clinical technique.

We have previously described an automated method for analysis of myocardial deformation that is feasible and time-saving, including automated segmentation, tracking the segment motion laterally using its speckle pattern and axially by tissue Doppler (8). The SR is measured by tissue Doppler, from the velocity gradient along a fixed distance along the ultrasound beam, and S is measured by the temporal integration of SR. In the segment length method, S and SR are measured directly by changes in segment length along the direction of the wall, not along the ultrasound beam, and thus are angle independent. We set up this study to evaluate the diagnostic accuracy of various

From the *Department of Circulation and Medical Imaging, Norwegian University of Science and Technology, Trondheim, Norway; and the †University of Queensland, Brisbane, Australia. This study was supported by grants from the Norwegian University of Science and Technology, Trondheim, Norway, and the National Health and Medical Research Council (project grant 210218), Canberra, Australia. Dr. Stoylen has received honoraria from GE Vingmed for lecturing, and both centers involved in this study have joint research studies with General Electric Medical Systems.

Manuscript received May 12, 2006; revised manuscript received December 12, 2006, accepted January 1, 2007.

Abbreviations and Acronyms

AUC = area under the curve
CAD = coronary artery disease
CX = circumflex artery
DSE = dobutamine stress echocardiography
LAD = left anterior descending artery
PSI = post-systolic strain index
ROC = receiver-operating characteristic
S = strain
S_{es} = end-systolic strain
S_{ps} = peak post-systolic strain
SR = strain rate
SR_s = peak systolic strain rate
SRI = strain rate imaging
t_{SRs} = time to peak systolic strain rate
WMS = wall motion score
WMSI = wall motion score index

deformation indexes as well as an automated segmental analysis method for SRI measurement, in patients undergoing DSE with normal or diseased coronary arteries and patients with low risk of coronary artery disease (CAD). The goal of this study was to evaluate the feasibility and diagnostic sensitivity of deformation imaging in DSE, including comparing the accuracy of various measurements by SRI with wall motion score (WMS) by 2-dimensional echo.

Methods

Study population. Dobutamine stress echocardiography was performed in 197 patients (age 58 ± 12 years, 98 women) at 2 centers. This sample size was selected to give an 80% power to identify a 10% improvement in the accuracy of wall motion scoring at a p value of 0.05. All patients had normal resting function (normal WMS at rest). Coronary angiography was performed within 6 months of DSE. Beta-adrenoceptor blockade was discontinued on the day before the test. Patients with left bundle branch block, cardiomyopathy, severe valvular heart disease, or ongoing atrial fibrillation/flutter were excluded. Patients who underwent the test for study purposes gave written informed consent, which was approved by the hospital ethics committees.

The clinical details of these patients are given in Table 1. The study population was divided into 60 patients at low probability (Framingham score <1%/year) of CAD who did not have coronary angiography, 61 patients with normal angiography, and 76 with >50% narrowing of at least 1 major vessel.

Dobutamine stress. A standard DSE protocol was performed with incremental dobutamine infusion rates of 5, 10, 20, 30, and 40 μg/kg/min every 3 min. Patients who did not achieve the target of 85% of the age-predicted maximal heart rate were given up to 2 mg of atropine until target heart rate was achieved. Criteria for terminating the test were completion of the protocol, severe ischemia evidenced by extensive new wall motion abnormalities, horizontal or downsloping ST-segment depression >2 mm, ST-segment elevation >1 mm in patients without prior myocardial infarction, severe angina, systolic blood pressure >240 or <100 mm Hg, serious ventricular arrhythmia, patient intolerance, or serious side effects caused by dobutamine.

Coronary angiography. Coronary angiography was performed using standard techniques, with an average interval between DSE and angiography of 41 days (range 1 to 170 days). The angiograms were evaluated by a single observer at each site, blinded to the echocardiographic results. Stenosis severity was measured by quantitative coronary angiography using an automated edge detection system (Philips Medical Systems, Eindhoven, the Netherlands). A maximal lumen diameter stenosis of >50% in any plane was classified as significant. Segmental disease was evaluated using a previously described 15-segment American Heart Association model of the coronary tree (9) to ensure that only stenoses in major epicardial vessels were assessed.

Echocardiography. IMAGE ACQUISITION. The examinations were performed with a Vivid 7 scanner (GE Vingmed Ultrasound, Horten, Norway) using a phased-array transducer. Three cine loops from the 3 standard apical planes (4-chamber, 2-chamber, and long-axis) were recorded in gray-scale harmonic mode and tissue Doppler mode simultaneously at baseline and peak stress. The pulse repetition frequency was between 1 and 1.5 kHz. The tissue Doppler frame rate ranged from 92/s to 225/s (mean 143/s), and 2-dimensional frame rate from 25/s to 70/s (mean 40/s). The number of tissue Doppler samples along each beam ranged from 122 to 296 (mean 181), but the number of

Table 1 Characteristics of Patients With Normal Angiography, With Low Probability of CAD, and With CAD (n = 197)

	Normal Coronary Angiography (n = 61)	Low Probability of CAD (n = 60)	CAD (n = 76)	p Value Normal vs. Low Probability	p Value Low Probability vs. CAD	p Value Normal vs. CAD
Age (yrs)	56 ± 12	53 ± 14	63 ± 9	0.4	<0.001	0.006
Diabetes	9 (14%)	6 (10%)	12 (16%)	0.4	0.3	0.9
Hypertension	22 (34%)	21 (35%)	27 (36%)	0.003	0.001	0.9
Hypercholesterolemia	33 (54%)	20 (33%)	51 (67%)	0.02	<0.001	0.1
Beta-blocker	32 (52%)	21 (34%)	55 (72%)	0.009	<0.001	0.02
Baseline systolic BP (mm Hg)	140 ± 23	133 ± 24	142 ± 21	0.3	0.07	0.8
Peak systolic BP (mm Hg)	146 ± 30	149 ± 27	141 ± 28	0.8	0.3	0.6
Baseline heart rate (beats/min)	67 ± 12	76 ± 11	63 ± 3	<0.001	<0.001	0.3
Peak heart rate (beats/min)	132 ± 16	142 ± 13	128 ± 17	0.06	<0.001	0.01

BP = blood pressure; CAD = coronary artery disease.

beams ranged from 8 to 24 (mean 15), giving a high axial but low lateral resolution. Echocardiographic data were stored digitally and subsequently analyzed offline.

ANALYSIS OF 2-DIMENSIONAL ECHOCARDIOGRAPHY. Regional wall motion analysis was assessed with a 16-segment model according to the American Society of Echocardiography by 2 experts blinded to the angiographic and patient data (10). Each segment was scored as: 1) normal, 2) hypokinetic, 3) akinetic, or 4) dyskinetic. The sum of WMSs, averaged over the number of segments with interpretive scores, gave the wall motion score index (WMSI). Ischemia was identified in the presence of new wall motion abnormality during DSE.

AUTOMATED IDENTIFICATION OF MYOCARDIAL SEGMENTS. For the automated measurements, we used a customized postprocessing system programmed in an engineering interface (GcMat, GE-Vingmed, Horten, Norway) that runs under Matlab (Math Works Inc., Natick, Massachusetts). This automated method of analyzing SRI has recently been described (8). In each apical view, the apex and mitral ring points were identified and the endocardial border was drawn automatically (11). The myocardium was divided into 6 equal segments, subject to manual adjustment. A speckle tracking method, using a pattern matching algorithm of the gray-scale data (12) combined with tissue Doppler velocities, was applied to kernels at the segment borders, enabling the motion of the myocardium to be followed in 2 dimensions throughout the cardiac cycle. Tracking was done axially (along the ultrasound beam) by tissue Doppler data, and laterally by speckle tracking. This search procedure resulted in tracking of segment position, segment orientation, and segment length throughout the cycle. The strain length (distance for velocity gradient calculation) was 10 to 15 mm for the tissue Doppler method, and axial averaging 1 mm and temporal averaging of 10 ms were used for the analysis.

AORTIC VALVE OPENING AND CLOSURE. The timing of aortic valve opening and closure were automatically defined by an algorithm developed at our department using tissue Doppler imaging (13,14). The SRI parameters were measured in 2 different ways, using either velocity data or segment length, but tracking was performed in the same way.

VELOCITY GRADIENT METHOD. A region of interest was placed automatically in the center of the segment at end-diastole, and the midpoint of the segment was tracked throughout the cardiac cycle. The SR was calculated from the velocity gradient along the ultrasound beam and strain was calculated as the temporal integral of SR, corrected from Eulerian SR to Lagrangian S, thus both being angle dependent.

SEGMENT LENGTH METHOD. Strain was calculated directly from the variation of the segment length using the tracked end points: strain = $(L - L_0)/L_0$. The SR was calculated as the temporal derivative of strain, with correction to Eulerian SR. This enabled angle-independent measurements of SR and strain. Segment tracking was done as in the velocity gradient method, and the segment was discarded if the speckle pattern region failed to track properly or if the gray-scale image showed regions with missing ultrasound data (dropouts) or larger reverberations. The displacement of the kernel region was used to check the tracking—ideally, this should be 0, because the kernel returns to the same baseline position by the end of the cardiac cycle. A displacement >2 mm indicated poor tracking. Figure 1 illustrates SR and S traces for both methods.

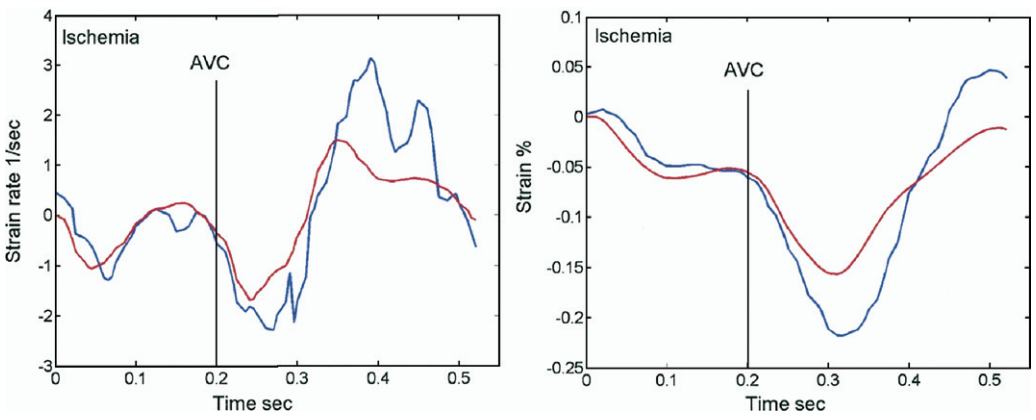

Figure 1 **Strain and Strain Rate Profiles With Automated Velocity and Segment Length Methods**

Strain rate and strain estimated with the 2 different methods (**red curve** = segment length method, **blue curve** = velocity gradient method). Strain rate traces are shown in the **left image**, and strain traces are shown in the **right image**. The traces are from a patient at peak dose showing ischemia in apical septum with low strain rate/strain values. The **traces in the lowest images** show postsystolic strain. Note the differences in the curves, the **red trace** has in general reduced value and a different shape compared with the **blue trace**. The red trace is smoother, probably because of lower temporal resolution. AVC = aortic valve closure.

MEASUREMENTS. Peak systolic strain rate (SR_s) was determined as the maximal negative SR value during ejection time, end systolic strain (S_{es}) as the magnitude of strain at aortic valve closure, and peak post-systolic strain (S_{ps}) as the greatest value after end systole. Delta SR and delta strain were measured as the difference between baseline and peak level values of DSE. Time to peak systolic strain rate (t_{SRs}) was measured from aortic valve opening to maximal negative SR value during ejection time. A post-systolic strain index (PSI) was calculated for all segments $(S_{ps} - S_{es})/S_{ps}$) (15). Coronary territories were identified as abnormal if any constituent segment had SR_s less than the specified minimum value (see the following text). All segments supplied by a stenosed coronary artery were labeled "at risk", and the presence of a minimum SR_s value less than the normal range defined the territory as abnormal.

Measurements were made in 18 segments from 3 apical views, for all 197 subjects, all blinded to the angiographic results. When SRI parameters were compared with the WMS, the 2 apical long-axis segments were deleted from the automated analysis to permit comparison in the 16 segments used for wall motion scoring.

Intraobserver and interobserver variability were tested in 20 randomly selected patients. We reanalyzed 18 segments from each, for a total 360 segments. The measurements were made at the same examinations, but not necessarily the same loop.

Derivation of cutoff values of SRI. DERIVATION OF CUTOFF VALUES. Patients with angiography were randomly divided; group A (n = 69) established a cutoff for the different parameters and group B (n = 68) tested the accuracy of the cutoff. To determine the clinical utility of the cutoffs, the sensitivity, specificity, and accuracy of WMS, SR_s, S_{es}, PSI, delta SR, delta S, and t_{SRs} in each patient and within each vascular territory (WMS, SR_s) were derived by cross-tabulation against the overall or regional results of coronary angiography. The defined cutoff values for ischemia at peak stress for the 6 parameters were applied for each segment, and patients were defined as having ischemia on the basis of having any number of abnormal segments within the 18 segments. The same system was applied on a vascular territory basis, and the presence of any abnormal segment within a vascular territory marked that territory as abnormal. A similar approach was used for visual wall motion scoring. Left ventricular wall segments were assigned to vascular territories as follows: left anterior descending artery (LAD); the entire apex, midseptum, basal and midanterior wall, basal and mid anteroseptum; left circumflex artery (CX); basal and midlateral wall, basal and midposterior wall; right coronary artery; basal septum and basal and midinferior wall. A fixed pattern of correspondence between coronary arteries and walls was used because of the difficulties in accounting for the exact coronary distribution.

Statistical analysis. Normalcy rate was examined as a referral bias-independent estimate of specificity, and was defined as the proportion of the 60 patients with a low pretest probability of CAD events (<1%/year) who had a normal response to DSE.

Measurements are presented as mean ± SD. Analysis of variance was used to compare continuous variables between groups, taking account of multiple segmental measurements and using the Scheffe method to correct for multiple comparisons. The Pearson chi-square test was used for the categorical data. The area under the receiver-operating characteristic (ROC) curve was used for comparison of sensitivity and specificity between methods. For comparison of the areas under the curves (AUCs) from paired ROCs, the standardized difference between the AUCs was used. The optimal ROC cut point was defined as the value having the highest sum of sensitivity and specificity. The McNemar test was used for paired categorical data, for example the pairwise comparison of sensitivity and specificity of WMS analysis against SR_s, S_{es}, PSI, delta SR, delta S, and t_{SRs} on a vascular and patient basis. Multiple regression analysis was used to establish that parameters were independent correlates of SR_s. The method of Bland and Altman was used for variability analysis. A value of $p < 0.05$ was considered statistically significant.

Results

Dobutamine echocardiography and coronary angiography. Table 1 summarizes the hemodynamic response to dobutamine stress. Target heart rate was achieved in 159 (81%) of the patients. In the remaining 39 patients, the protocol was terminated at a submaximal heart rate because of severe ischemia or side effects (hypotension, hypertension, ventricular arrhythmia, patient intolerance), or inability to attain target heart rate despite dobutamine and atropine.

Of the 76 patients with coronary stenoses, 35 (46%) had single-vessel disease, 31 (41%) had 2-vessel disease, and 10 (13%) had 3-vessel disease. A significant stenosis was present in the LAD in 49 patients (65%), in the left CX in 31 patients (41%), and in the right coronary artery in 42 patients (55%). Only 2 of the patients had a left dominant system.

Feasibility of deformation analysis. In all, 3,546 myocardial segments were analyzed. The segment length method yielded the greatest number of analyzable segments both for SR_s and S_{es} at baseline and peak compared with the velocity gradient method. Visual wall motion assessment had a significantly higher feasibility compared with the SRI methods ($p < 0.001$). The feasibility of WMS at baseline was 99%, significantly higher ($p < 0.001$) than 86% for SR_s and 79% for S_{es} by the segment length method, and 80% for SR_s and 65% for S_{es} by the velocity gradient method. At peak, the feasibility was 98% for WMS, but still significantly higher ($p < 0.001$) than 84% for SR_s and 77% for S_{es} by the segment length method, and 80% for SR_s and 65% for S_{es} by the velocity gradient method. There were no significant differences between baseline and peak for any of the 3

Table 2 Intraobserver and Interobserver Variability for SR_s at Baseline and Peak for Velocity Gradient and Segment Length Methods

	Velocity Gradient, Rest	Velocity Gradient, Peak	Segment Length, Rest	Segment Length, Peak
Intraobserver COV (%)	10	15	13	17
Total mean SR_s (s^{-1})	−1.27	−2.34	−1.17	−2.11
Range	−1.32 to −1.22	−2.50 to −2.17	−1.22 to −1.13	−2.21 to −2.03
95% limits of agreement	−0.23, 0.28	−0.62, 0.80	−0.29, 0.29	−0.75, 0.75
Bias	0.02	0.09	0	0
Interobserver COV (%)	16	25	17	22
Total mean, SR_s (s^{-1})	−1.28	−2.30	−1.14	−2.05
Range	−1.33 to −1.22	−2.48 to −2.21	−1.20 to −1.11	−2.14 to −1.97
95% limits of agreement	−0.42, 0.42	−1.18, 1.23	−0.42, 0.39	−0.8, 1.0
Bias	0.01	0.02	0.01	0.10

COV = coefficient of variation; SR_s = peak systolic strain rate.

methods. The differences between the segment length and velocity gradient methods were all significant ($p = 0.001$).

The interobserver and intraobserver variability was tested in 10 patients (180 segments) and is shown in Table 2.

ROC curves for cutoff values and accuracy. Figure 2 illustrates the results of the ROC analysis for group A for the 6 parameters, and Figure 3 summarizes sensitivity, specificity, and accuracy for group B for the 3 parameters with the highest AUC. The greatest area under the ROC curve to distinguish the presence or absence of CAD (0.90 for both velocity gradient and segment length methods) was obtained for SR_s for both methods (Fig. 2), significantly exceeding the areas for S_{es} ($p < 0.001$). The AUCs were significantly lower for PSI, delta S, and t_{SRs} ($p < 0.001$) and not significantly different for the rest.

The optimal cutoffs for peak SR_s were >-1.3 and $-1.2\ s^{-1}$ for velocity gradient and segment length, which gave a sensitivity of 84% and 86%, specificity of 93% and 89%, and accuracy of 87% and 87%, respectively. For WMS for the same group, sensitivity was 72% ($p = 0.02$), specificity 87% ($p = 1.0$), and accuracy 78% ($p = 0.17$). Use of the cutoffs in group B gave an accuracy of 90% for the velocity gradient method and 87% for the segment length method. Peak SR_s and S_{es} did not differ with respect to accuracy to identify CAD for either method (Fig. 3). The WMS for this group showed a sensitivity of 73% ($p = 0.02$), specificity of 81% ($p = 0.69$), and accuracy of 76% ($p = 0.07$).

The following cutoffs were derived for the remaining velocity gradient and segment length parameters from group A: $S_{es} > -9\%$ and -8%; PSI > 0.27 and 0.30; delta SR < 0.1 and 0.1; delta S < -9 and -8, and $t_{SRs} > 0.115$ ms and 0.125 ms. On the basis of sensitivity and specificity, the results for peak SR_s and S_{es} were analogous (Fig. 3). For the velocity gradient method, the sensitivity of PSI was significantly lower than SR_s ($p = 0.04$), and for specificity, delta SR ($p = 0.02$) and delta S ($p = 0.0002$) were significantly lower. The specificity was lower for delta S ($p = 0.02$) compared with SR_s in the segment length method. In patients with a low probability of CAD, normalcy of SR_s using the same cutoff was 82%.

Segments at risk, SRs (velocity gradient method) compared with WMSI. The SR_s at peak stress was significantly greater in the normal segments ($-2.6 \pm 0.8\ s^{-1}$) compared with the segments at risk ($-2.3 \pm 1.1\ s^{-1}$) ($p < 0.001$). By WMS, 177 segments were classified as ischemic with a mean SR_s of $-0.8 \pm 0.2\ s^{-1}$. The same applied to single-vessel disease using minimum SR_s with a value of $-1.7 \pm 0.4\ s^{-1}$ in the normal segments and $-1.1 \pm 0.6\ s^{-1}$ in the segments at risk ($p < 0.001$). The sensitivity in single-vessel disease by minimum SR_s value was 78% compared with 68% for WMSI. The sensitivity for multivessel disease was 92% for minimum SR_s ($-0.85\ s^{-1}$) and 80% for WMSI.

Comparison of WMS (expert reading of gray-scale data) and SR_s for detecting CAD and coronary territory. The sensitivity, specificity, and accuracy of WMS and the SR techniques in all patients are compared in Figure 4. The WMS was less sensitive, but the techniques showed similar specificity and overall accuracy. The sensitivity for single-vessel disease was 68% with WMS compared with 81% and 80% for velocity gradient and segment length ($p = 0.12$). For the identification of disease in patients with multivessel disease, the sensitivity of WMS was 82%, not significantly different from 92% for velocity gradient SR_s and 89% with segment length SR_s ($p = 0.22$). The ability to recognize the involvement of more than 1 vessel in multivessel disease was 49% for SR_s (velocity gradient), 50% for SR_s (segment length), and 42% for WMS ($p = 0.16$).

The sensitivity for WMS and SR_s for the velocity gradient method and the segment length method were compared for the 3 main coronary arteries in 35 patients with single-vessel disease, including 16 with disease in the LAD, 9 in the CX, and 10 in the right coronary artery. Sensitivity was highest in the LAD territory with the automated methods (88% for velocity gradient method and 87% for segment length method) compared with wall motion analysis (75%). Wall motion analysis

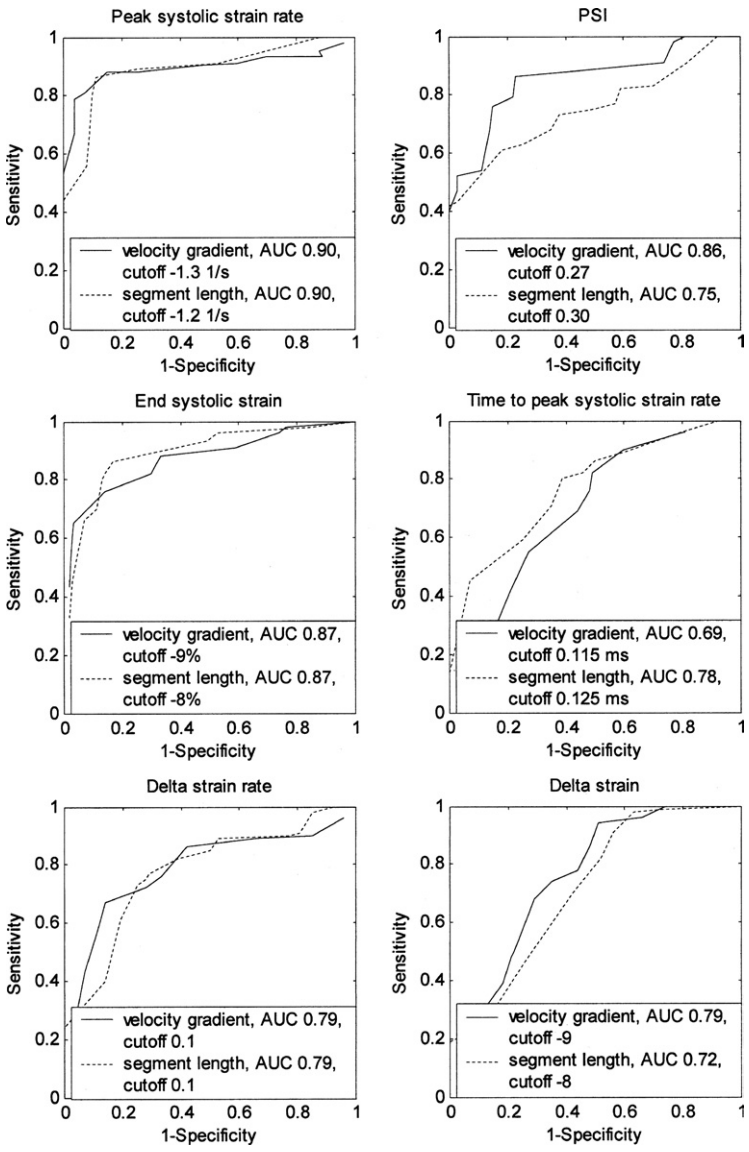

Figure 2 **Receiver-Operating Characteristic Curves and Optimal Cutoff Points for Various Deformation Indexes**

The receiver-operating characteristic curves and area under the curve (AUC) at peak dobutamine stress echocardiography for peak systolic strain rate, post-systolic strain index (PSI), end systolic strain, delta strain, delta strain rate, and time to peak systolic strain rate for velocity gradient and segment length methods.

showed the lowest sensitivity (56%, p = 0.5) in the left CX and was highest for the velocity gradient method (78%) followed by the segment length method (77%). The right coronary artery showed similar sensitivity of 80% for all 3 methods.

Detection of disease in individual coronary arteries. The LAD supplied 49 territories with a sensitivity by WMS of 61% compared with 82% for the velocity gradient method and 76% for the segment length method. The left CX supplied 31 territories, and the sensitivities for WMS, velocity gradient method, and segment length method were 62%, 65%, and 46%, respectively. The right coronary artery supplied 42 territories, with WMS having a sensitivity of 77%, compared with 56% for the velocity gradient method and 60% for the segment length method.

Discussion

The results of this study document the feasibility of an automated method for quantifying SRI at peak DSE, by either the velocity gradient or the segment length method. These findings increased the sensitivity of DSE compared with expert conventional reading.

Definition of abnormal range. We defined the optimal cutoff for abnormal range from the coronary angiography

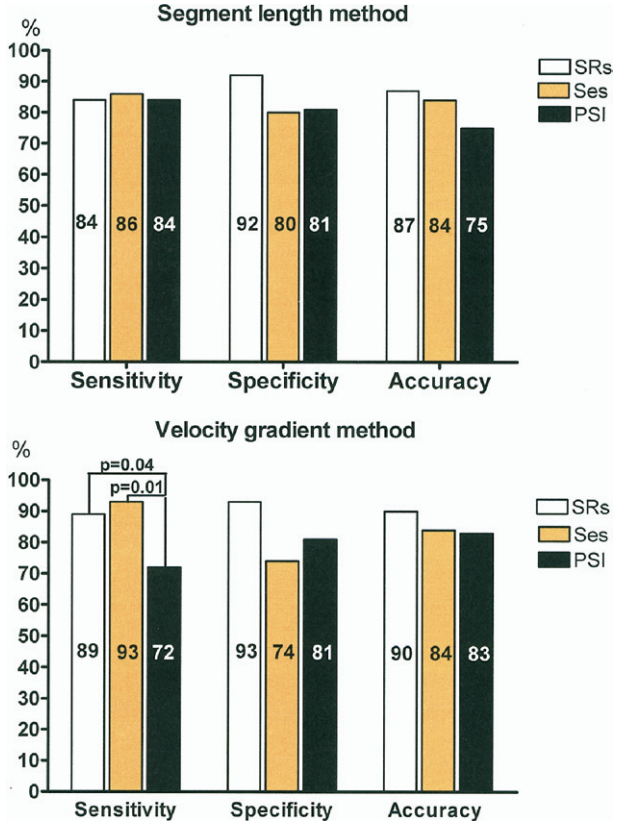

Figure 3 **Accuracy of Stress Deformation Parameters for Diagnosis of CAD**

The sensitivity, specificity, and accuracy of the 3 most important strain rate imaging parameters during peak stress are shown in the 2 figures for the patients with coronary angiography. Values for the segment length method and the velocity gradient method are given in the 2 figures. The sensitivity, specificity, and accuracy for the optimal cutoffs values are based on receiver-operating characteristics curves in group A and are evaluated here in group B. CAD = coronary artery disease; PSI = postsystolic strain index; S_{es} = end-systolic strain; SR_s = peak systolic strain rate.

group A, which designated as abnormal any SR value >-1.3 for the velocity gradient method and -1.2 s^{-1} for the segment length method.

There was no significant difference for either method between the normal group and the low probability group at peak stress for SR_s or S_{es}, indicating that the normalcy rate was a referral bias-independent estimate of specificity.

Detection of coronary disease. The use of SR_s and S_{es} in this study permitted a higher sensitivity than was obtainable with WMS for an expert reader. The diagnostic accuracy of DSE depends on several factors: the threshold for defining significant CAD (extent and severity), the criteria for a positive test, the presence or absence of prior infarction, and referral bias. Groups with a high prevalence of multivessel coronary disease and previous myocardial infarction are more likely to develop ischemia in response to stress (16). The accuracy of WMS in this study (77%) was slightly lower than in earlier studies, in which a sensitivity of 81% and a specificity of 80% were reported (16), and this probably reflects the selection of patients without infarction (17). Posttest referral bias might tend to increase the sensitivity in patients among whom angiography was performed after the patient had undergone a positive test (18), but only 28% of patients were in this group.

The process of attributing myocardium to coronary territories is inexact, potentially influenced by collaterals, and difficult in patients with stenoses of intermediate severity. The angiographic model was used to define the location of the stenoses in the main coronary arteries; the 15-segment angiographic model and the 16-segment echocardiographic model do not correspond. To simplify the imprecise process of defining segmental accuracy, we approximated a fixed pattern between coronary arteries and the myocardial segments they supplied, recognizing that this could make the regional specificity appear worse than it actually was.

Detection of single-vessel disease and recognition of multivessel disease. The detection of single-vessel disease with DSE can be challenging with standard interpretation, with reported sensitivities averaging 66% (range 10% to 91%) (19). In this study, the sensitivity was 68% for WMS and 81% for SR_s, and the lack of significant difference likely reflected a relatively small number of patients with single-vessel disease. Detection of left CX disease was poor for WMS, concordant with earlier studies showing a mean sensitivity of 55% (20), probably most attributable to poor resolution of the lateral wall. Importantly, the performance of SR_s was also poor in the posterior circulation, with sensitivity being highest in the LAD territory.

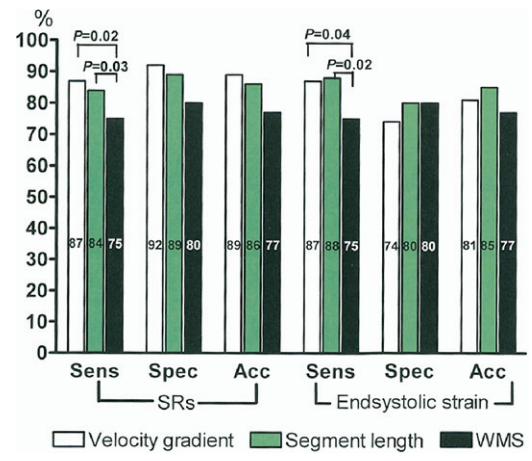

Figure 4 **Comparison of Accuracy of SR_s and Strain With WMS**

Wall motion score (WMS) and peak systolic strain rate are compared for velocity gradient and segment length methods in 136 patients with an angiogram. Sensitivity (Sens), specificity (Spec), and accuracy (Acc) are compared as well as the sensitivity for the 3 main coronary arteries in single-vessel disease (n = 35): left main artery (n = 16), circumflex artery (n = 9), and right coronary artery (n = 10). SR_s = peak systolic strain rate.

Although stress echocardiography is a sensitive technique for the recognition of multivessel disease in patients with previous myocardial infarction (20), it is much more difficult to recognize the involvement of more than 1 territory in a patient with normal resting function, with sensitivities more in the order of 50% (16). Both WMS and SR techniques in this study had a sensitivity of 40% to 50% for this purpose, supporting the contention that patients are limited by the onset of ischemia, thus detecting mainly the area with the lowest ischemic threshold, and this represents an inherent limitation of using wall motion irrespective of method, rather than perfusion reserve (21). However, the inability to detect multivessel disease as well as perfusion-based methods might not be as great a limitation as it might seem, because most patients with positive examinations for ischemia subsequently undergo cardiac catheterization.

Selection of the optimal SRI parameter. Our study showed the optimal parameters of stress-induced ischemia to be SR_s, with an AUC of 0.90 for both velocity gradient and segment length techniques and end-systolic strain with an AUC of 0.87 for both velocity gradient and segment length techniques. Minimum SR_s was used to characterize segments as normal or abnormal, and gave a higher sensitivity compared with WMS. End-systolic strain also showed a significantly higher sensitivity compared with WMS.

Earlier experimental studies have suggested SR to be a better quantitative parameter for DSE compared with strain, based on the association of SR with regional contractile function (or dP/dt) rather than the association between strain and ventricular geometry (22). However, Voigt et al. (7,23) have reported postsystolic index, a marker of postsystolic thickening, to offer the optimal results (AUC 0.95). The reason for this disparity is unclear; conceivably, the automated process for selection of the velocity gradient-based SRI curves was based on optimizing the SR profile, and this may have compromised the S_{es} profile. From the standpoint of speckle tracking, the use of a lower frame rate (which is necessary to optimize tracking of the speckle signal) may compromise the ability to gather timing data. Although the change in SR might be expected to offer the greatest accuracy for identifying ischemia, this did not perform as well as SR_s, possibly reflecting the potential for combining errors from both measurements.

Study limitations. Coronary angiography was used as the reference standard in this study; although widely accepted for this purpose, some discrepancies arise from the comparison of coronary anatomy and physiology. Coronary lesion severity can be overestimated and underestimated by angiography, and the physiological effect of stenoses varies with site, length, and vessel size.

The balance between adequate frame rate (temporal resolution) and the number of beams (spatial resolution) is an ongoing issue with important implications (24). Overemphasis on temporal resolution results in the use of too few beams, with low spatial resolution in the basal segments, leading to the possibility of contamination of the tissue signal by Doppler shifts from the ventricular blood pool. The temporal resolution of speckle tracking is a particularly difficult balance between undersampling at low frame rate (leading to lower peak values and difficulty with tracking the speckle pattern because of excessive change from one frame to the next) and reduced line density at a high frame rate, compromising lateral resolution and giving poor transverse tracking. This study included a range of frame rate and line density for the gray-scale and tissue Doppler data, reflecting an increasing understanding of the importance of these settings in the course of acquiring these data. The combined acquisition of tissue Doppler and B-mode represents a compromise from optimal settings of each, and acquisitions at the range of frame rate may have compromised the feasibility and accuracy of the segment length method.

Although we applied an automated method of SRI measurement, this does not yet allow entirely objective assessment of regional myocardial function. There remains a need for an educated user to overcome the limitations of Doppler-derived deformation analysis. Angle deviation, reverberations, drop-outs, and misalignment have to be taken into consideration when accepting or rejecting a curve. Speckle tracking has limitations because of the dependence on good image quality for the gray-scale data. Tissue Doppler has disadvantages concerning reverberations, angle deviation, and noise (random and nonrandom). Thus, the SRI curve still requires interpretation in the context of the gray-scale image, and uncritical use of SRI data may be misleading if the image is of poor quality and especially if the SRI waveform is suboptimal.

Conclusions

The results of this study confirm that SRI with both segment length and velocity gradient techniques is feasible during DSE. Automated analysis seems more practicable than manual analysis on the basis of time requirement, at the cost of a small reduction in feasibility. In this study, automated SRI measurement increased the sensitivity of DSE compared with expert conventional reading. Therefore, automated SRI may be a valuable supplement to wall motion scoring when analyzing DSE in the clinical setting.

Acknowledgment
The authors thank Dr. Knut Bjornstad, who contributed to the wall motion analysis.

Reprint requests and correspondence: Dr. Thomas H. Marwick, University of Queensland, School of Medicine, Princess Alexandra Hospital, Brisbane, QLD 4102, Australia. E-mail: tmarwick@uq.edu.au.

REFERENCES

1. Picano E, Lattanzi F, Orlandini A, Marini C, L'Abbate A. Stress echocardiography and the human factor: the importance of being expert. J Am Coll Cardiol 1991;17:666–9.

2. Cain P, Baglin T, Khoury V, Case C, Marwick T. Automated regional myocardial displacement for facilitating the interpretation of dobutamine echocardiography. Am J Cardiol 2002;89:1347–53.
3. Cain P, Marwick T, Case C, et al. Assessment of regional long-axis function during dobutamine echocardiography. Clin Sci 2001;100: 423–32.
4. Cain P, Short L, Baglin T, Case C, Bosch H, Marwick T. Development of a fully quantitative approach to the interpretation of stress echocardiography using radial and longitudinal myocardial velocities. J Am Soc Echocardiogr 2002;15:759–67.
5. Fathi R, Cain P, Nakatani S, Yu H, Marwick T. Effect of tissue Doppler on the accuracy of novice and expert interpreters of dobutamine echocardiography. Am J Cardiol 2001;88:400–5.
6. Fraser A, Payne N, Madler C, et al. Feasibility and reproducibility of off-line tissue Doppler measurement of regional myocardial function during dobutamine stress echocardiography. Eur J Echocardiogr 2003; 4:43–53.
7. Voigt J, Nixdorff U, Bogdan R, et al. Comparison of deformation imaging and velocity imaging for detecting regional inducible ischaemia during dobutamine stress echocardiography. Eur Heart J 2004;25:1517–25.
8. Bjork Ingul C, Torp H, Aase S, Berg S, Stoylen A, Slordahl S. Automated analysis of strain rate and strain; feasibility and clinical implications. J Am Soc Echocardiogr 2005;18:410–7.
9. Austen WG, Edwards JE, Frye RL, et al. A reporting system on patients evaluated for coronary artery disease. Report of the Ad Hoc Committee for Grading of Coronary Artery Disease, Council on Cardiovascular Surgery, American Heart Association. Circulation 1975;51 Suppl:5–40.
10. Lang RM, Bierig M, Devereux RB, et al. Recommendations for chamber quantification: a report from the American Society of Echocardiography's Guidelines and Standards Committee and the Chamber Quantification Writing Group, developed in conjunction with the European Association of Echocardiography, a branch of the European Society of Cardiology. J Am Soc Echocardiogr 2005;18:1440–63.
11. Torp AH, Rabben SI, Stoylen A, et al. Automatic detection and tracking of left ventricular landmarks in echocardiography. Proc IEEE Ultrasonics Symp 2004;1:474–7.
12. Bohs L, Trahey G. A novel method for angle independent ultrasonic imaging of blood flow and tissue motion. IEEE Trans Biomed Eng 1991;38:280–6.
13. Aase S, Stoylen A, Bjork Ingul C, Frigstad S, Torp H. Automatic timing of aortic valve closure in apical tissue Doppler images. Ultrasound Med Biol 2006;32:19–27.
14. Aase S, Stoylen A, Ingul C, Frigstad S, Torp H. Automated detection of aortic valve closure in apical tissue Doppler images. Proc IEEE Ultrasonics Symp 2004;3:2061–4.
15. Kukulski T, Jamal F, Herbots L, et al. Identification of acutely ischemic myocardium using ultrasonic strain measurements. A clinical study in patients undergoing coronary angioplasty. J Am Coll Cardiol 2003;41:810–9.
16. Marwick T. Stress echocardiography. Heart 2003;89:113–8.
17. Marcovitz P, Armstrong W. Accuracy of dobutamine stress echocardiography in detecting coronary artery disease. Am J Cardiol 1992;69: 1269–73.
18. Krenning B, Geleijnse M, Poldermans D, Roelandt J. Methodological analysis of diagnostic dobutamine stress echocardiography studies. Echocardiography 2004;21:725–36.
19. Marwick TH. Accuracy of stress echocardiography. In: Stress Echocardiography: Its Role in the Diagnosis and Evaluation of Coronary Artery Disease. Norwell, MA: Kluwer Academic Publishers, 2003: 76–7.
20. Geleijnse M, Fioretti P, Roelandt J. Methodology, feasibility, safety and diagnostic accuracy of dobutamine stress echocardiography. J Am Coll Cardiol 1997;30:595–606.
21. Moir S, Haluska BA, Jenkins C, Fathi R, Marwick TH. Incremental benefit of myocardial contrast to combined dipyridamole-exercise stress echocardiography for the assessment of coronary artery disease. Circulation 2004;110:1108–13.
22. Weidemann F, Jamal F, Kowalski M, et al. Can strain rate and strain quantify changes in regional systolic function during dobutamine infusion, beta-blockade, and atrial pacing—implications for quantitative stress echocardiography. J Am Soc Echocardiogr 2002; 15:416–24.
23. Voigt JU, Exner B, Schmiedehausen K, et al. Strain-rate imaging during dobutamine stress echocardiography provides objective evidence of inducible ischemia. Circulation 2003;107:2120–6.
24. Hanekom L, Lundberg V, Leano R, Marwick T. Optimisation of strain rate imaging for application to stress echocardiography. Optimisation of strain rate imaging for application to stress echocardiography. Ultrasound Med Biol 2004;30:1451–60.